

STOCHASTIC MODELS WITH NON-GAUSSIAN FORCE DISTRIBUTIONS IN COARSE-GRAINING MOLECULAR DYNAMICS

SP.VENKAT REDDY¹| P.NARESH KUMAR²| PASULAVARI VIKAS³|
BANGARI VAISHNAVI⁴

1&2 Associate Professor, Maths department, Brilliant Grammar School Educational Society's Group of Institutions, Hyderabad, TS.

3&4 UG SCHOLARS, Maths department, Brilliant Grammar School Educational Society's Group of Institutions, Hyderabad, TS.

Abstract

Because activities occurring at the atomic and cellular levels occur on very different spatial and temporal scales, it is difficult to incorporate atomistic and molecule information into models of cellular behavior. Molecular dynamics (MD) and coarse-grained models in various cell regions are used in multiscale or multi-resolution approaches to overcome this challenge. The precision and characteristics of the coarse-grained model, which approximates the comprehensive MD description, determine their usefulness. Written as relatively low-dimensional systems of nonlinear stochastic differential equations, a family of stochastic coarse-grained (SCG) models is introduced. The non-Gaussian force distribution seen in MD simulations that linear models are unable to capture is incorporated into the nonlinear SCG model. Detailed MD simulations demonstrate that the nonlinearities can be selected so as not to complicate the parametrization of the SCG description. Gamma functions are used to find the solution to the SCG model.

Keywords :multiscale modelling · coarse-graining · molecular dynamics · Brownian dynamics

1 Introduction

The need to include microscopic data (from X-ray crystallography, NMR spectroscopy, or cryo-electron microscopy)

into dynamical models of intracellular processes has grown as experimental knowledge of the atomic or near-atomic structure of biomolecules and intracellular components has increased. Molecular dynamics (MD) simulations based on classical molecular mechanics are a popular method. The positions and velocities of individual atoms in these MD models are expressed as rather large systems of ordinary or stochastic differential equations, which may also be subject to algebraic constraints (Leimkuhler and Matthews, 2015; Lewars, 2016). While there have been reports in the literature of all-atom MD simulations of systems with a million atoms (Tarasova et al., 2017; Farafanov and Nerukh, 2019), these simulations are limited to comparatively narrow computational domains, up to tens of nanometers in length. Modern computers cannot replicate intracellular activities, such as the movement of molecules over micrometers, as doing so would necessitate simulating trillions of atoms (Erban and Chapman, 2019).

Although BD models or their multi-resolution extensions simulate individual molecules of chemical species involved, the binding of Ca²⁺ ions to channel sites or other interactions between molecules are only described using relatively coarse probabilistic approaches. For example, the BD model of Dobramysl et al. (2016) describes interactions in terms of reaction radii and binding probabilities as

implemented by Erban and Chapman (2009) and Lipkov'a et al. (2011). Atomic-level information is not included in BD models. In order to use this information, multi-resolution methodologies have to consider MD simulations in parts of the simulation domain. In the case of ions, such a multi-resolution scheme has been developed by Erban (2016), where an all-atom MD model of ions in water is coupled with a stochastic coarsegrained (SCG) description of ions in the rest of the computational domain. The accuracy and efficiency of such multi-resolution methodologies depend on the quality of the SCG description of the underlying MD model. In this paper, we present and analyze a class of SCG models which can be used to fit non-Gaussian distributions estimated from all-atom MD simulations. While the velocity distribution of the coarse-grained particle can be well approximated by a Gaussian (normal) distribution in our MD simulations, this is not the case of the force distribution. Non-Gaussian force distributions have also been reported by Shin et al. (2010) and Carof et al. (2014) in their MD simulations of particles in Lennard-Jones fluids. Thus our SCG model is formulated in a way which incorporates a Gaussian distribution for the velocity and a non-Gaussian distribution for the force (acceleration).

Given an integer $N \geq 1$, a coarse-grained particle (for example, an ion) will be described by $(2N + 2)$ three-dimensional variables: its position X , velocity V and $2N$ auxiliary variables U_j and Z_j , where $j = 1, 2, \dots, N$. Denoting $X \equiv (X_1, X_2, X_3)$, $V \equiv (V_1, V_2, V_3)$, $U_j \equiv (U_{j,1}, U_{j,2}, U_{j,3})$ and $Z_j \equiv (Z_{j,1}, Z_{j,2}, Z_{j,3})$, the time evolution of the SCG model is given by

$$dX_i = V_i dt, \quad \text{for } i = 1, 2, 3, \quad (2)$$

$$dV_i = \sum_{j=1}^N U_{j,i} dt, \quad (3)$$

$$dU_{j,i} = (-\eta_{j,1} V_i + h_j(Z_{j,i})) g'_j(g_j^{-1}(U_{j,i})) dt, \quad \text{for } j = 1, 2, \dots, N, \quad (4)$$

$$dZ_{j,i} = -(\eta_{j,2} h_j(Z_{j,i}) + \eta_{j,3} U_{j,i}) dt + \eta_{j,4} dW_{j,i}, \quad (5)$$

where $g_j : \mathbb{R} \rightarrow \mathbb{R}$ is an increasing differentiable function, g'_j is its derivative, g_j^{-1} is its inverse, $h_j : \mathbb{R} \rightarrow \mathbb{R}$ is a continuous function and $\eta_{j,k}$ are positive constants for $j = 1, 2, \dots, N$ and $k = 1, 2, 3, 4$. We note that some of our assumptions on g_j can be relaxed as long as $g'_j(g_j^{-1}(U_{j,i}))$ appearing in equation (4) can be suitably defined.

The SCG description (2)–(5) includes $2N$ functions g_j and h_j and $4N$ additional parameters $\eta_{j,k}$, which can be all adjusted to fit properties of the detailed all-atom MD model. In particular the SCG model (2)–(5) can better match the MD trajectories of ions than the BD description given by equation (1), which only has one parameter, diffusion constant D , to fit to the MD results.

One of the shortcomings of equation (1) is that its derivation from the underlying MD model requires us to consider the limit of sufficiently large times. In particular, we need to discretize equation (1) with a relatively large.

time step, say a nanosecond, to use it as a description of the trajectory of an ion. Since the typical time step of an all-atom MD model is a femtosecond, it is difficult to design a multi-resolution scheme which would replace all-atom MD simulations by equation (1) in parts of the computational domain. The SCG model (2)–(5) can be used to fit not only the diffusion constant D but other important properties of all-atom MD models, which improves the accuracy of the SCG model at time steps comparable with the MD timestep.

SCG models can be constructed using a relatively automated procedure by postulating that an ion interacts with

additional ‘fictitious particles’. Such a methodology has been applied to coarse-grained modelling of biomolecules by Davtyan et al. (2015, 2016) to improve the fit between an MD model and the dynamics on a coarse-grained potential surface. They use fictitious particles with harmonic interactions with coarse-grained degrees of freedom (i.e. they add quadratic terms to the potential function of the system and linear terms to equations of motions) and each fictitious particle is also subject to a friction force and noise. An application of such an approach to ions leads to systems of linear stochastic differential equations (SDEs) and can be used, after some transformation, to obtain a simplified version of the SCG model (2)–(5), where functions g_j and h_j are given as identities, i.e. $g_j(y) = h_j(y) = y$ for $y \in \mathbb{R}$ and $j = 1, 2, \dots, N$. Using this simplifying assumption in the SCG model (2)–(5), we obtain

$$\frac{dX_i}{dt} = V_i, \quad \text{for } i = 1, 2, 3, \quad (6)$$

$$\frac{dV_i}{dt} = \sum_{j=1}^N U_{j,i} \frac{dU_{j,i}}{dt}, \quad (7)$$

$$\frac{dU_{j,i}}{dt} = (-\eta_{j,1} V_i + Z_{j,i}) \frac{dZ_{j,i}}{dt}, \quad \text{for } j = 1, 2, \dots, N, \quad (8)$$

$$\frac{dZ_{j,i}}{dt} = -(\eta_{j,2} Z_{j,i} + \eta_{j,3} U_{j,i}) \frac{dU_{j,i}}{dt} + \eta_{j,4} dW_{j,i}. \quad (9)$$

This is a linear system of SDEs with $4N$ parameters. It has been shown by Erban (2016) that such models can fit an increasing number of properties of all-atom MD simulations as we increase N . For example, the linear SCG model (6)–(9) can be used to fit the diffusion constant D and second moments of the velocity and the force for $N = 1$, while the velocity autocorrelation function can better be fitted for larger values of N , e.g. for $N = 3$. However, there are other properties of MD simulations which cannot be captured by linear models even if consider arbitrarily large N . They include, for example, all distributions which are not Gaussian. This motivates the introduction of general

functions h_j and g_j in the SCG model (2)–(5).

Considering the SCG model (2)–(5) in its full generality, it can capture more interesting dynamics. However, coarse-grained models can only be useful if they can be easily parametrized. Thus in our analysis, we focus on choices of functions g_j and h_j which both improve the properties of the SCG description and do not complicate its analysis and parametrization. The rest of the paper is organized as follows. In Section 2, we consider the linear SCG model (6)–(9) for $N = 1$, which is followed in Section 3 with the analysis of the linear model for general values of N . To get some further insights into the properties of this model, we study its connections with the corresponding generalized Langevin equation. In Section 4, we consider the nonlinear SCG model (2)–(5) for $N = 1$. We consider specific choices of nonlinearity g_1 , for which the model can be solved in terms of incomplete gamma functions. This helps us to design three approaches to parametrize the nonlinear SCG model, which are applied to data obtained from MD simulations. We conclude with the analysis of the nonlinear SCG model (2)–(5) for general values of N in Section 5.

2 Linear model for $N = 1$ and the generalized Langevin equation

We begin by considering the linear SCG model (6)–(9) for $N = 1$. To simplify our notation in this section, we will drop some subscripts and denote $X = X_1$, $V = V_1$, $U = U_{1,1}$, $Z = Z_{1,1}$, $W = W_{1,1}$ and $\eta_k = \eta_{1,k}$ for $k = 1, 2, 3, 4$. Then equations (6)–(9) read as follows

$$dX = V dt, \quad (10)$$

$$dV = U dt, \quad (11)$$

$$dU = (-\eta_1 V + Z) dt, \quad (12)$$

$$dZ = -(\eta_2 Z + \eta_3 U) dt + \eta_4 dW, \quad (13)$$

where X is (one coordinate of) the position of the coarse-grained particle (ion), V is its velocity, U is its acceleration, Z is an auxiliary variable, dW is white noise and η_j , $j = 1, 2, 3, 4$, are positive parameters. In order to find the values of four parameters η_j suitable for modelling ions, Erban (2016) estimates the diffusion constants D and three second moments $\langle V^2 \rangle$, $\langle U^2 \rangle$ and $\langle Z^2 \rangle$ from allatom MD simulations of ions (K^+ , Na^+ , Ca^{2+} and Cl^-) in aqueous solutions. The four parameters of the SCG model (10)–(13) can then be chosen as

$$\eta_1 = \frac{\langle U^2 \rangle}{\langle V^2 \rangle}, \quad \eta_2 = \frac{\langle Z^2 \rangle}{D} \left(\frac{\langle V^2 \rangle}{\langle U^2 \rangle} \right)^2, \quad \eta_3 = \frac{\langle Z^2 \rangle}{\langle U^2 \rangle}, \quad \eta_4 = \sqrt{\frac{2}{D} \frac{\langle V^2 \rangle \langle Z^2 \rangle}{\langle U^2 \rangle}}. \quad (14)$$

Then the SCG model (10)–(13) gives the same values of D , $\langle V^2 \rangle$, $\langle U^2 \rangle$ and $\langle Z^2 \rangle$ as obtained in all-atom MD simulations.

Since the model (10)–(13) only has four parameters, we can only hope to get the exact match of four quantities estimated from all-atom MD. To get some insights into what we are missing, we will derive the corresponding generalized Langevin equation and study its consequences. The generalized Langevin equation can be written in the form

$$\frac{dV}{dt} = - \int_0^t K(\tau) V(t - \tau) d\tau + R(t), \quad (15)$$

where $K : [0, \infty) \rightarrow \mathbb{R}$ is a memory kernel and random term $R(t)$ satisfies the generalized fluctuation-dissipation theorem, given below in equation (21). To derive the generalized Langevin equation (15), consider the two-variable subsystem (12)–(13) of the SCG model. Denoting $y = (U, Z)^T$, where T stands for transpose, equations (12)–(13) can be written in vector notation as follows

$$dy = B y dt + b_1 V dt + b_2 dW, \quad (16)$$

where matrix $B \in \mathbb{R}^{2 \times 2}$ and vectors $b_j \in \mathbb{R}^2$, $j = 1, 2$, are given as

$$B = \begin{pmatrix} 0 & 1 \\ -\eta_3 & -\eta_2 \end{pmatrix}, \quad b_1 = \begin{pmatrix} -\eta_1 \\ 0 \end{pmatrix} \quad \text{and} \quad b_2 = \begin{pmatrix} 0 \\ \eta_4 \end{pmatrix}.$$

Let us denote the eigenvalues and eigenvectors of B as λ_j and $v_j = (1, \lambda_j)^T$, $j = 1, 2$, respectively. The eigenvalues of B are the solutions of the characteristic polynomial $\lambda^2 + \eta_2 \lambda + \eta_3 = 0$. They are given by

$$\lambda_1 = -\frac{\eta_2}{2} + \mu \quad \text{and} \quad \lambda_2 = -\frac{\eta_2}{2} - \mu \quad \text{where} \quad \mu = \sqrt{\frac{\eta_2^2}{4} - \eta_3}. \quad (17)$$

Since η_2 and η_3 are positive parameters, we conclude that real parts of both eigenvalues are negative. In what follows, we will assume $\eta_2^2 \geq 4\eta_3$. Then we have two distinct eigenvalues and the general solution of the SDE system (16) can be written as follows

$$y(t) = \Phi(t) c + \Phi(t) \int_0^t \Phi^{-1}(s) b_1 V(s) ds + \Phi(t) \int_0^t \Phi^{-1}(s) b_2 dW, \quad (18)$$

where $c \in \mathbb{R}^2$ is a constant vector determined by initial conditions and matrix $\Phi(t) \in \mathbb{R}^{2 \times 2}$ is given as

$$\Phi(t) = (\exp(\lambda_1 t) v_1 \mid \exp(\lambda_2 t) v_2) = \begin{pmatrix} \exp(\lambda_1 t) & \exp(\lambda_2 t) \\ \lambda_1 \exp(\lambda_1 t) & \lambda_2 \exp(\lambda_2 t) \end{pmatrix},$$

i.e. each column is a solution of the ODE system $dy = B y dt$. Calculating the inverse of $\Phi(t)$ and considering long-time behaviour, equation (18) simplifies to

$$U(t) = - \int_0^t K(\tau) V(t - \tau) d\tau + R(t), \quad (19)$$

where memory kernel $K(\tau)$ is given by

$$K(\tau) = \frac{\eta_1}{\lambda_1 - \lambda_2} (\lambda_1 \exp(\lambda_2 \tau) - \lambda_2 \exp(\lambda_1 \tau)) \quad (20)$$

and noise term $R(t)$ is Gaussian with zero mean and the equilibrium correlation function satisfying the generalized fluctuation-dissipation theorem in the form

$$\langle R(t_1) R(t_2) \rangle = \frac{\eta_4^2}{2\eta_1 \eta_2 \eta_3} K(t_2 - t_1). \quad (21)$$

Using (17), memory kernel (20) can be rewritten as

$$K(\tau) = \eta_1 \exp\left(-\frac{\eta_2 \tau}{2}\right) \left(\cosh(\mu \tau) + \frac{\eta_2}{2\mu} \sinh(\mu \tau) \right), \quad (22)$$

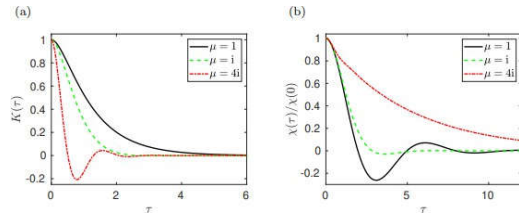


Fig. 1 (a) Memory kernel $K(\tau)$ given by equation (22) for $\eta_1 = 1$, $\eta_2 = 4$ and three different values of η_3 , namely $\eta_3 = 3$ (solid line, $\mu = 1$), $\eta_3 = 5$ (dashed line, $\mu = i$) and $\eta_3 = 20$ (dot-dashed line, $\mu = 4i$). (b) Normalized velocity autocorrelation function $\chi(\tau)/\chi(0)$ computed by using equation (25) for the same parameter values as in panel (a).

where $\mu = \sqrt{\eta_2^2/4 - \eta_3}$. We note that the auxiliary coefficient μ is a square root of a real negative number for $\eta_2^2/4 < 4\eta_3$. However, formula (22) is still valid in this case: for $\eta_2^2/4 < 4\eta_3$ it can be rewritten in terms of sine and cosine functions, taking into account that $\mu = i|\mu|$ is pure imaginary, $\sinh(i|\mu|\tau) = i\sin(|\mu|\tau)$ and $\cosh(i|\mu|\tau) = \cos(|\mu|\tau)$. The memory kernel $K(\tau)$, given by equation (22), is plotted in Figure 1(a) for different values of parameter μ . For simplicity, we use non-dimensionalized versions of our equations with dimensionless parameters $\eta_1 = 1$ and $\eta_2 = 4$. We choose three different values of η_3 so that the values of μ are 1, i and $4i$. In Figure 1(b), we plot the equilibrium velocity autocorrelation function which is defined as

$$\chi(\tau) = \lim_{t \rightarrow \infty} \langle V(t) V(t - \tau) \rangle,$$

for $\tau \in [0, \infty)$. More precisely, we plot $\chi(\tau)/\chi(0)$ which is normalized so that its value at $\tau = 0$ is equal to 1. It is related to the memory kernel by

$$\frac{\chi(\tau)}{\chi(0)} = \mathcal{L}^{-1} \left(\frac{1}{s + \mathcal{L}[K](s)} \right), \quad (23)$$

where $\mathcal{L}[K](s) = \int_0^\infty K(\tau) \exp(-s\tau) d\tau$ is the Laplace transform of the memory kernel $K(\tau)$ and \mathcal{L}^{-1} denotes Laplace inversion. Following Erban and Chapman (2019), we evaluate the right hand side of equation (23) as follows. Substituting equation (22) into (23), we obtain

$$\frac{\chi(\tau)}{\chi(0)} = \mathcal{L}^{-1} \left(\frac{s^2 + \eta_2 s + \eta_3}{s^3 + \eta_2 s^2 + (\eta_1 + \eta_3)s + \eta_1 \eta_2} \right). \quad (24)$$

The polynomial in the denominator, $p(s) = s^3 + \eta_2 s^2 + (\eta_1 + \eta_3)s + \eta_1 \eta_2$, has positive coefficients. Since $p(-\eta_2) < 0 < p(0)$, it has one negative real root in interval $(-\eta_2, 0)$, which we denote by a_1 . The other two roots (a_2 and a_3 say) may be real or complex, but if they are complex they will be complex conjugates since $p(s)$ has real coefficients. Assuming that the real part of each root is negative, we first find the partial fraction decomposition of the rational function in (24) as

$$\frac{s^2 + \eta_2 s + \eta_3}{s^3 + \eta_2 s^2 + (\eta_1 + \eta_3)s + \eta_1 \eta_2} = \frac{c_1}{s - a_1} + \frac{c_2}{s - a_2} + \frac{c_3}{s - a_3},$$

where $c_i \in \mathbb{C}$ are constants (which depend on η_1 , η_2 and η_3). Then we can rewrite (23) as

$$\frac{\chi(\tau)}{\chi(0)} = c_1 \exp(a_1 \tau) + c_2 \exp(a_2 \tau) + c_3 \exp(a_3 \tau). \quad (25)$$

The results computed by (25) are shown in Figure 1(b). We note that although equation (25) may include complex exponentials, the resulting $\chi(\tau)$ is always real. Since the diffusion constant, D , and the second moment of the equilibrium velocity distribution, $\langle V^2 \rangle$, are related to χ by

$$D = \int_0^\infty \chi(\tau) d\tau = \frac{\eta_1^2}{2\eta_1^2 \eta_2^2} \quad \text{and} \quad \langle V^2 \rangle = \chi(0) = \frac{\eta_1^2}{2\eta_1 \eta_2 \eta_3},$$

the parametrization (14) guarantees that both the value of $\chi(0)$ and the integral of $\chi(\tau)$ are captured accurately. However, the simplified SCG description (10)–(13) is not suitable to perfectly fit the velocity

autocorrelation function or the memory kernel for all values of $\tau \in [0, \infty)$. In order to do this, we have to consider the SCG model (6)–(9) for larger values of N as it is done in the following section.

3 General linear SCG model and autocorrelation functions

Considering the linear SCG model (6)–(9) for general values of N , we can solve equations (8)–(9) for each value of $j = 1, 2, \dots, N$ to generalize our previous result (19) as

$$U_{j,i}(t) = - \int_0^t K_j(\tau) V_i(t - \tau) d\tau + R_{j,i}(t), \quad (26)$$

where kernel $K_j(\tau)$ is given by (compare with (22))

$$K_j(\tau) = \eta_{j,1} \exp\left(-\frac{\eta_{j,2}\tau}{2}\right) \left(\cosh(\mu_j \tau) + \frac{\eta_{j,2}}{2\mu_j} \sinh(\mu_j \tau) \right) \quad (27)$$

With

$$\mu_j = \sqrt{\frac{\eta_{j,2}^2}{4} - \eta_{j,3}} \quad (28)$$

and noise term $R_{j,i}(t)$ is Gaussian with zero mean and the equilibrium correlation function satisfying

$$\langle R_{j,i}(t_1) R_{j,i}(t_2) \rangle = \frac{\eta_{j,4}^2}{2 \eta_{j,1} \eta_{j,2} \eta_{j,3}} K_j(t_2 - t_1).$$

Substituting (26) to (7), we obtain the generalized Langevin equation

$$\frac{dV_i}{dt} = - \int_0^t K(\tau) V_i(t - \tau) d\tau + R_i(t), \quad (29)$$

Where

$$K(\tau) = \sum_{j=1}^N K_j(\tau) \quad \text{and} \quad R_i(t) = \sum_{j=1}^N R_{j,i}(t). \quad (30)$$

In particular, we have $3N$ parameters to fit memory kernel $K(\tau)$, which can be estimated from all-atom MD simulations. There have been a number of approaches developed in the literature to estimate the

memory kernel from MD simulations. Shin et al. (2010) use an integral equation with relates memory kernel $K(\tau)$ with the autocorrelation function for the force and the correlation function between the force and the velocity. Estimating these correlation functions from long time MD simulations and solving the integral equation, they obtain memory kernel $K(\tau)$. Other methods to estimate the memory kernel, $K(\tau)$, of the corresponding generalized Langevin equation (29) have been presented by Gottwald et al. (2015) and Jung et al. (2017). An alternative approach to parametrize the linear SCG model (6)–(9) is to estimate the velocity autocorrelation function, $\chi(\tau)$, from all-atom MD simulations. This can be done by computing how correlated is the current velocity (at time t) with velocity at previous times. Since equations (10)–(13) are linear SDEs, we can follow Mao (2007) to solve them analytically, using eigenvalues and eigenvectors of matrices appearing in their corresponding matrix formulation. Using this analytic solution, Erban (2016) use an acceptance-rejection algorithm to fit the parameters of linear SCG model (6)–(9) for $N = 3$ to match the velocity autocorrelation functions of ions estimated from all-atom MD simulations of Na^+ and K^+ in the SPC/E water. Since the parameter μ_j given by (28) is a square root of a real number, it can be both positive or purely imaginary. In particular, kernels $K_j(\tau)$ given by equation (27) can include both exponential, sine and cosine functions as illustrated in Figure 1(a). Since memory kernel $K(\tau)$ is given as the sum of $K_j(\tau)$ in equation (30), typical memory kernels and correlation functions estimated from all-atom MD simulations can be successfully matched by linear SCG models for relatively small values of N . However, as shown by Mao (2007), analytic solutions of linear SDEs also

imply that the process is Gaussian at any time $t > 0$, provided that we start with deterministic initial conditions. Thus the linear SCG model (6)–(9) for arbitrary values of N can only fit distributions which are Gaussian. This motivates our investigation of the nonlinear SCG model in the next two sections.

4 Nonlinear SCG model for $N = 1$

We begin by considering the nonlinear SCG model (2)–(5) for $N = 1$. As in Section 2, we simplify our notation by dropping some subscripts and denoting $X = X_i$, $V = V_i$, $U = U_{1,i}$, $Z = Z_{1,i}$, $W = W_{1,i}$, $g = g_j$, $h = h_j$ and $\eta_k = \eta_{1,k}$ for $k = 1, 2, 3, 4$. Then equations (2)–(5) read as follows

$$dX = V dt, \quad (31)$$

$$dV = U dt, \quad (32)$$

$$dU = (-\eta_1 V + h(Z)) g'(g^{-1}(U)) dt, \quad (33)$$

$$dZ = -(\eta_2 h(Z) + \eta_3 U) dt + \eta_4 dW, \quad (34)$$

where X denotes (one coordinate of) the position of the coarse-grained particle, V is its velocity, U is its acceleration, Z is an auxiliary variable, dW is white noise, η_j , for $j = 1, 2, 3, 4$, are positive parameters and functions $g : \mathbb{R} \rightarrow \mathbb{R}$ and $h : \mathbb{R} \rightarrow \mathbb{R}$ are yet to be specified.

Equation (31) describes the time evolution of the position, while equations (32)–(34) admit a stationary distribution. We denote it by $p(v, u, z)$. Then $p(v, u, z) dv du dz$ gives the probability that $V(t) \in [v, v+dv)$, $U(t) \in [u, u+du)$ and $Z(t) \in [z, z+dz)$ at equilibrium. The stationary distribution, $p(v, u, z)$, of SDEs (32)–(34) can be obtained by solving the corresponding stationary Fokker-Planck equation

$$\frac{\eta_1^2}{2} \frac{\partial^2 p}{\partial^2 z}(v, u, z) = \frac{\partial}{\partial v} (u p(v, u, z)) + \frac{\partial}{\partial u} ((-\eta_1 v + h(z)) g'(g^{-1}(u)) p(v, u, z)) + \frac{\partial}{\partial z} ((-\eta_2 h(z) - \eta_3 u) p(v, u, z)),$$

which give

$$p(v, u, z) = \frac{C}{g'(g^{-1}(u))} \exp \left[-\frac{2\eta_2}{\eta_1^2} \left(\eta_1 \eta_3 \frac{v^2}{2} + \eta_3 G(g^{-1}(u)) + H(z) \right) \right], \quad (35)$$

) where C is the normalization constant, and functions G and H are integrals of functions g and h , respectively, which are given

$$G(y) = \int_0^y g(\xi) d\xi \quad \text{and} \quad H(y) = \int_0^y h(\xi) d\xi. \quad (36)$$

) We note that for the special case where g and h are given as identities, i.e. $g(y) = h(y) = y$ for $y \in \mathbb{R}$, the nonlinear SCG model (31)–(34) is equal to the linear SCG model (10)–(13) and functions G and H are $G(y) = H(y) = y^2/2$. Then the stationary distribution (35) is product of Gaussian distributions in v , u and z variables. In particular, we can easily calculate the second moments of these distributions in terms of parameters η_j . Estimating these moments from all-atom MD simulations, we can parametrize the resulting linear SCG model (10)–(13) as shown in equation (14). However, if we want to match a non-Gaussian force distribution, we have to consider nonlinear models. A simple one-parameter example is studied in the next section.

4.1 One-parameter nonlinear function

Consider that g is a function depending on one additional positive parameter η_5 as follows

$$g(y) = |y|^{1/\eta_5} \text{sign } y, \quad (37)$$

where we use sign to denote the sign (signum) function

$$\text{sign } y = \begin{cases} -1, & \text{for } y < 0, \\ 0, & \text{for } y = 0, \\ 1, & \text{for } y > 0. \end{cases} \quad (38)$$

The function defined by (37) only satisfies our assumptions on g for $\eta_5 \in (0, 1]$ as it is not differentiable at $y = 0$ for $\eta_5 > 1$, but we will proceed with our analysis for any positive $\eta_5 > 0$. Consider that function h is an identity, i.e. $h(y) = y$ for $y \in \mathbb{R}$, then equations (31)–(34) reduce to

$$dX = V dt, \quad (39)$$

$$dV = U dt, \quad (40)$$

$$dU = (-\eta_1 V + Z) \eta_5^{-1} |U|^{1-\eta_5} dt, \quad (41)$$

$$dZ = -(\eta_2 Z + \eta_3 U) dt + \eta_4 dW, \quad (42)$$

where we would have to be careful, if we used this model to numerically simulate trajectories for $\eta_5 > 1$, because of possible division by zero for $U = 0$ in equation (41). If $\eta_5 \in (0, 1]$, then we do not have such technical issues. Using equation (35), the stationary distribution is equal to

$$p(v, u, z) = C |u|^{\eta_5-1} \exp \left[-\frac{\eta_2}{\eta_4} \left(\eta_1 \eta_3 v^2 + \frac{2\eta_3 \eta_5}{1+\eta_5} |u|^{1+\eta_5} + z^2 \right) \right], \quad (43)$$

where the normalization constant is given by

$$\int_{-\infty}^{\infty} \int_{-\infty}^{\infty} \int_{-\infty}^{\infty} p(v, u, z) dv du dz = 1.$$

Integrating (43), we get

$$C = \frac{\eta_2 \sqrt{\eta_1 \eta_3}}{\pi \eta_4^2} \left(\frac{\eta_2 \eta_3 \eta_5}{\eta_4^2} \right)^{\eta_5/(1+\eta_5)} \left(\frac{1+\eta_5}{2} \right)^{1/(1+\eta_5)} \frac{1}{\Gamma\left(\frac{\eta_5}{1+\eta_5}\right)},$$

where Γ is the gamma function defined as

$$\Gamma(s) = \int_0^{\infty} \xi^{s-1} \exp(-\xi) d\xi. \quad (44)$$

Let $\alpha \geq 0$. Integrating (43), we get

$$\langle |U|^\alpha \rangle = \left(\frac{\eta_4^2 (1+\eta_5)}{2\eta_2 \eta_3 \eta_5} \right)^{\alpha/(1+\eta_5)} \frac{\Gamma\left(\frac{\alpha+\eta_5}{1+\eta_5}\right)}{\Gamma\left(\frac{\eta_5}{1+\eta_5}\right)}. \quad (45)$$

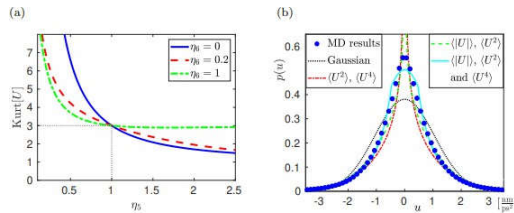


Fig. 2 (a) Kurtosis $\text{Kurt}[U]$ given by equation (59) as a function of parameter η_5 for three different values of parameter η_6 . The result for $\eta_6 = 0$ (blue solid line) corresponds to the case of one-parameter function g , defined by (37), where the kurtosis is given by (46). (b) Distribution of U estimated from a long-time MD simulation (blue circles) compared with

the results obtained by the linear SCG model (10)–(13) (black dotted line), nonlinear SCG models (31)–(34) with one-parameter function g , defined by (37), fitting hU^2 i and hU^4 i (red dot-dashed line) and $h|U|i$ and hU^2 i (green dashed line), and the nonlinear SCG model (31)–(34) with two-parameter function g defined by (52), matching all three moments $h|U|i$, hU^2 i and hU^4 i (cyan solid line).

Using (45) for $\alpha = 2$ and $\alpha = 4$, we obtain the following expression for kurtosis

$$\text{Kurt}[U] = \frac{\langle U^4 \rangle}{\langle U^2 \rangle^2} = \Gamma\left(\frac{\eta_5}{1+\eta_5}\right) \Gamma\left(\frac{4+\eta_5}{1+\eta_5}\right) \left(\Gamma\left(\frac{2+\eta_5}{1+\eta_5}\right) \right)^{-2}. \quad (46)$$

In particular, the kurtosis is only a function of one parameter, η_5 . It is plotted in Figure 2(a) as the blue solid line, together with the kurtosis obtained for a more general two-parameter SCG model studied in Section 4.2. We observe that the distribution of U is leptokurtic for $\eta_5 < 1$ and platykurtic for $\eta_5 > 1$. If η_5 is equal to 1, then our SCG model given by equations (31)–(34) reduces to the linear SCG model given by equations (10)–(13), i.e. the stationary distribution is Gaussian and its kurtosis is 3. This is shown by the dotted line in Figure 2(a).

Since equation (46) only depends on parameter η_5 , we can use the kurtosis of the acceleration distribution (which is equal to the kurtosis of the force distribution) estimated from MD simulations to find the value of parameter η_5 . To calculate the kurtosis, we estimate the fourth moment hU^4 i in addition to the second moment, hU^2 i, used before in our estimating procedure (14) for the linear model. In particular, we not only get equation (46) for calculating the value of parameter η_5 , but also a restriction on other parameters η_2 , η_3 and η_4 . Using (45) for $\alpha = 2$, it can be stated as follows

$$\frac{\eta_4^2}{2\eta_2\eta_3} = \frac{\eta_5}{1+\eta_5} \left(\frac{1+\eta_5}{\pi} \sin\left(\frac{\pi}{1+\eta_5}\right) (U^2)^{(1+\eta_5)/2} \left(\Gamma\left(\frac{\eta_5}{1+\eta_5}\right) \right)^{1+\eta_5} \right), \quad (47)$$

where we have used properties of the gamma function, including $\Gamma(1+y) = y\Gamma(y)$ and Euler's reflection formula, $\Gamma(1-y)\Gamma(y) \sin(\pi y) = \pi$, to simplify the right hand side. We note that in the Gaussian case, $\eta_5 = 1$, the right hand side of equation (47) further simplifies to

$$\frac{\eta_4^2}{2\eta_2\eta_3} = \langle U^2 \rangle, \quad (48)$$

which is indeed the formula for the second moment of U given by the linear SCG model (10)–(13). Equation (47) provides one restriction on four remaining parameters, η_1 , η_2 , η_3 and η_4 , which need to be specified. This can be done by estimating three additional statistics from MD simulations, as in the case of the linear SCG model (10)–(13) in equation (14). Indeed, the stationary distributions of V and Z are Gaussian with mean zero. Their second moments and the diffusion constant, D , for the nonlinear SCG model (31)–(34) can be calculated as

$$D = \frac{\eta_4^2}{2\eta_1^2\eta_2^2}, \quad \langle V^2 \rangle = \frac{\eta_4^2}{2\eta_1\eta_2\eta_3} \quad \text{and} \quad \langle Z^2 \rangle = \frac{\eta_4^2}{2\eta_2}. \quad (49)$$

Therefore, assuming that D , $hV/2$, $hZ/2$ are obtained from MD simulations and $\eta_4/2(2\eta_2\eta_3)$ is given by (47), we can calculate parameters η_k by

$$\eta_1 = \frac{1}{\langle V^2 \rangle} \left(\frac{\eta_4^2}{2\eta_2\eta_3} \right), \quad \eta_2 = \frac{\langle Z^2 \rangle \langle V^2 \rangle^2}{D} \left(\frac{\eta_4^2}{2\eta_2\eta_3} \right)^{-2}, \quad (50)$$

$$\eta_3 = \langle Z^2 \rangle \left(\frac{\eta_4^2}{2\eta_2\eta_3} \right)^{-1}, \quad \eta_4 = \sqrt{\frac{2}{D} \langle Z^2 \rangle \langle V^2 \rangle} \left(\frac{\eta_4^2}{2\eta_2\eta_3} \right)^{-1}. \quad (51)$$

We note that in the Gaussian case, $\eta_5 = 1$, we can substitute equation (48) for $\eta_4/2(2\eta_2\eta_3)$ and the parametrization approach (50)–(51) simplifies to equation (14) used in the case of the linear SCG model (10)–(13). In the next subsection, we generalize formula (37) to a two-parameter function and show that the parametrization approach (50)–(51) is still

applicable to the case of more general SCG models.

4.2 Two-parameter nonlinear function

Consider that g is a function depending on two positive parameters η_5 and η_6 as follows

$$g(y) = \begin{cases} 0, & \text{for } |y| \leq \eta_6^{1-\eta_5}, \\ \left(\eta_6 \left(1 - \frac{1}{\eta_5} \right) + \frac{\eta_6^{1-\eta_5}}{\eta_5} |y| \right) \text{sign } y, & \text{for } \eta_6^{1-\eta_5} < |y| \leq \eta_6^{1-\eta_5}, \\ |y|^{1/\eta_5} \text{sign } y, & \text{for } |y| > \eta_6^{1-\eta_5}, \end{cases} \quad (52)$$

where sign function is defined by (38). In particular, our expression for function g is equal to the formula (37) for sufficiently large values of $|y|$. As discussed in the previous section, if we used formula (37), there would be some issues for y close to zero (for example, the division by zero for $U = 0$ and $\eta_5 > 1$ in equation (41)), so our generalized formula (52) replaces (37) with a linear function for smaller values of $|y|$. On the face of it, it looks that there could also be some issues with the generalized formula (52), because it is not strictly increasing for $|y| \leq \eta_6^{1-\eta_5}$. However, function (52) is increasing and invertible away of this region with its inverse given by

$$g^{-1}(u) = \begin{cases} \eta_5 \eta_6^{1-\eta_5} \left(|u| - \eta_6 \left(1 - \frac{1}{\eta_5} \right) \right) \text{sign } u, & \text{for } 0 < |u| \leq \eta_6, \\ |u|^{\eta_5} \text{sign } u, & \text{for } |u| > \eta_6. \end{cases}$$

Moreover, what we really need in equations (31)–(34) is $g'(g^{-1}(u))$ which can be defined as the following continuous function

$$g'(g^{-1}(u)) = \frac{1}{\eta_5} \times \begin{cases} \eta_6^{1-\eta_5}, & \text{for } |u| \leq \eta_6, \\ |u|^{1-\eta_5}, & \text{for } |u| > \eta_6, \end{cases} \quad (53)$$

where the removable discontinuity at $u = 0$ has disappeared because we have defined $g'(g^{-1}(0)) = \eta_6^{1-\eta_5}/\eta_5$. Integrating (52) and substituting (53), we get

$$G(g^{-1}(u)) = \begin{cases} \frac{\eta_5 \eta_6^{1-\eta_5}}{2} u^2, & \text{for } |u| \leq \eta_6, \\ \frac{\eta_5 (\eta_5 - 1) \eta_6^{1-\eta_5}}{2(1+\eta_5)} + \frac{\eta_5}{1+\eta_5} |u|^{1+\eta_5}, & \text{for } |u| > \eta_6, \end{cases} \quad (54)$$

where G is the integral of function g defined by (36). Consider again that h is an identity, i.e. $h(y) = y$ for $y \in \mathbb{R}$. Then the stationary distribution (35) is again Gaussian in V and Z variables with their second moments given by equation (49). Let us denote the marginal stationary distribution of U by

$$p_u(u) = \int_{-\infty}^{\infty} \int_{-\infty}^{\infty} p(v, u, z) dv dz.$$

Using (35) and (54), we have

$$p_u(u) = \begin{cases} C_u \eta_6^{\eta_5-1} \exp \left[-\frac{\eta_2 \eta_3 \eta_5 \eta_6^{1+\eta_5}}{\eta_4^2} \left(\frac{u^2}{\eta_6^2} + \frac{1-\eta_5}{1+\eta_5} \right) \right], & \text{for } |u| \leq \eta_6, \\ C_u |u|^{\eta_5-1} \exp \left[-\frac{2\eta_2 \eta_3 \eta_5}{\eta_4^2 (1+\eta_5)} |u|^{1+\eta_5} \right], & \text{for } |u| > \eta_6, \end{cases} \quad (55)$$

where C_u is the normalization constant given by

$$\int_{-\infty}^{\infty} p_u(u) du = 1.$$

Let us define

$$\kappa_1 = \frac{\eta_2 \eta_3 \eta_5 \eta_6^{1+\eta_5}}{\eta_4^2} \quad \text{and} \quad \kappa_2 = \frac{1}{1+\eta_5}. \quad (56)$$

Integrating (55), we get, for any $\alpha \geq 0$,

$$\frac{\langle |U|^\alpha \rangle}{\eta_6^\alpha} = \frac{F(\kappa_1, \kappa_2, \alpha)}{F(\kappa_1, \kappa_2, 0)}, \quad (57)$$

where function $F(\kappa_1, \kappa_2, \alpha)$ is defined by

$$F(\kappa_1, \kappa_2, \alpha) = (2\kappa_1 \kappa_2)^{(1-\alpha)\kappa_2} \exp(2\kappa_1 \kappa_2) \Gamma(1 + (\alpha-1)\kappa_2, 2\kappa_1 \kappa_2) + \kappa_1^{(1-\alpha)/2} \exp(\kappa_1) \gamma\left(\frac{\alpha+1}{2}, \kappa_1\right) \quad (58)$$

and Γ (resp. γ) is the upper (resp. lower) incomplete gamma function defined by

$$\Gamma(s, y) = \int_y^\infty \xi^{s-1} \exp(-\xi) d\xi, \quad \gamma(s, y) = \int_0^y \xi^{s-1} \exp(-\xi) d\xi.$$

Substituting $\alpha = 2$ and $\alpha = 4$ in equation (57), we get

$$\text{Kurt}[U] = \frac{\langle U^4 \rangle}{\langle U^2 \rangle^2} = \frac{F(\kappa_1, \kappa_2, 4) F(\kappa_1, \kappa_2, 0)}{(F(\kappa_1, \kappa_2, 2))^2}. \quad (59)$$

This formula for the kurtosis is visualized in Figure 2(a) as a function of parameter η_5 for three different values of parameter η_6 . We note that the case $\eta_6 = 0$ corresponds to the case studied in Section 4.1. If $\eta_6 = 0$, then equation (56) implies $\kappa_1 = 0$. Since $\gamma(s, 0) = 0$ and $\Gamma(s, 0) = \Gamma(s)$, where $\Gamma(s)$ is the standard gamma function given by (44), we can confirm that equation (59) converges to our previous result (46) as $\eta_6 \rightarrow 0$. Substituting $\alpha = 1$ into (58), we obtain $F(\kappa_1, \kappa_2, 1) = \exp(\kappa_1)$. Consequently, using $\alpha = 1$ in equation (57), we obtain

$$\frac{\langle |U| \rangle}{\eta_6} = \frac{\exp(\kappa_1)}{F(\kappa_1, \kappa_2, 0)}. \quad (60)$$

Using $\alpha = 2$ in equation (57), we get

$$\frac{\langle U^2 \rangle}{\langle |U| \rangle^2} = \frac{F(\kappa_1, \kappa_2, 2) F(\kappa_1, \kappa_2, 0)}{\exp(2\kappa_1)}. \quad (61)$$

Consequently, if we use MD simulations to estimate not only the second and fourth moments, $\langle U^2 \rangle$ and $\langle U^4 \rangle$, but also the first absolute moment $\langle |U| \rangle$, we can substitute the estimated MD values into equations (59) and (61) to obtain two equations for two unknowns κ_1 and κ_2 . Solving these two equations numerically, we can get κ_1 and κ_2 . Then we can use (56) and (60) to get the original parameters η_5 and η_6 by

$$\eta_5 = \frac{1-\kappa_2}{\kappa_2} \quad \text{and} \quad \eta_6 = \frac{\langle |U| \rangle F(\kappa_1, \kappa_2, 0)}{\exp(\kappa_1)}. \quad (62)$$

Moreover, equation (56) also implies the following restriction on other parameters η_2, η_3 and η_4

$$\frac{\eta_4^2}{\eta_2 \eta_3} = \frac{1-\kappa_2}{\kappa_1 \kappa_2 \exp(\kappa_1/\kappa_2)} \left(\langle |U| \rangle F(\kappa_1, \kappa_2, 0) \right)^{1/\kappa_2}. \quad (63)$$

This restriction is equivalent to restriction (47). Therefore, assuming again that D, hV_2 and hZ_2 are obtained from MD simulations and $\eta_2/4/(2\eta_2\eta_3)$ is given by (63), we can calculate parameters η_1, η_2 ,

η_3 and η_4 by equations (50)–(51). We note that the two additional parameters η_5 and η_6 can be used to satisfy both equations (59) and (61), while in Section 4.1 we could only use one equation (equation (46) for kurtosis) to fit one parameter η_5 . However, in the case of one-parameter function (37), we could (instead of fitting the kurtosis) match the quantity hU^2 with MD simulations, i.e. we could replace equation (46) by equation (61) simplified to the one-parameter case corresponding to function (37). Passing to the limit $\eta_6 \rightarrow 0$ in equation (61) and using Euler's reflection formula, $\Gamma(1 - y)\Gamma(y) \sin(\pi y) = \pi$, we obtain that the one-parameter nonlinearity (37) implies the following formula

$$\frac{\langle U^2 \rangle}{\langle |U| \rangle^2} = \frac{\pi}{1 + \eta_5} \left(\sin \left(\frac{\pi}{1 + \eta_5} \right) \right)^{-1}. \quad (64)$$

Thus, in Section 4.1, we could use $h|U|$ and hU^2 estimated from long-time MD simulations to calculate the left hand side of equation (64), which could then be used to select parameter η_5 . Other parameters could again be chosen by equations (50)–(51).

5 Nonlinear SCG model for general values of N

We have already observed in Sections 2 and 3 that the linear SCG model (6)–(9) can match the MD values of a few moments for $N = 1$, while we need to consider larger values of N to match the entire velocity autocorrelation function. Considering the nonlinear SCG model (2)–(5), we have two options to capture more details of the non-Gaussian force distribution observed in MD simulations. We could either keep $N = 1$, as in Section 4, and introduce additional parameters into nonlinearity $g = g_1$, or we could consider larger values of N . In Section 4, we have shown that by going from one-parameter

to two-parameter function g , we improve the match with MD results. In this section, we will discuss the second option: we will use larger values of N . Consider equations corresponding to the i -coordinate, $i = 1, 2, 3$, of the nonlinear SCG model (2)–(5). Let us denote the stationary distribution of equations (3)–(5) by

$$p(v, \mathbf{u}, \mathbf{z}) \equiv p(v, u_1, u_2, \dots, u_N, z_1, z_2, \dots, z_N).$$

Then $p(v, u, z) dv du_1 du_2 \dots du_N dz_1 dz_2 \dots dz_N$ gives the probability that $V_i(t) \in [v, v + dv)$, $U_{j,i}(t) \in [u_j, u_j + du_j)$ and $Z_{j,i}(t) \in [z_j, z_j + dz_j)$, for $j = 1, 2, \dots, N$, at equilibrium. The stationary distribution can be obtained by solving the corresponding stationary Fokker-Planck equation

$$\begin{aligned} \frac{\eta_{j,4}^2}{2} \frac{\partial^2 p}{\partial^2 z_j}(v, \mathbf{u}, \mathbf{z}) &= \frac{\partial}{\partial v} \left(p(v, \mathbf{u}, \mathbf{z}) \sum_{j=1}^N u_j \right) \\ &+ \sum_{j=1}^N \frac{\partial}{\partial u_j} \left((-\eta_{j,1}v + h_j(z_j)) g_j'(g_j^{-1}(u_j)) p(v, \mathbf{u}, \mathbf{z}) \right) \\ &+ \sum_{j=1}^N \frac{\partial}{\partial z_j} \left((-\eta_{j,2}h_j(z_j) - \eta_{j,3}u_j) p(v, \mathbf{u}, \mathbf{z}) \right). \end{aligned} \quad (65)$$

Our analysis in Section 4.1 shows that parameters $\eta_{j,2}$, $\eta_{j,3}$ and $\eta_{j,4}$ appear on the left hand side of equation (47) as a suitable fraction, which in the Gaussian case corresponds to the second moment of the acceleration (see equation (48)). Considering general N , we define this fraction as new parameters.

$$\sigma_j = \frac{\eta_{j,4}^2}{2 \eta_{j,2} \eta_{j,3}}, \quad \text{for } j = 1, 2, \dots, N,$$

and we again assume that the second moment of the velocity distribution, hV^2 can be estimated from long-time MD simulations. In order to find the stationary distribution, we will require that parameters $\eta_{j,1}$, $\eta_{j,2}$, $\eta_{j,3}$ and $\eta_{j,4}$ satisfy (compare with equation (49) for $N = 1$)

$$\langle V^2 \rangle = \frac{\eta_{j,4}^2}{2 \eta_{j,1} \eta_{j,2} \eta_{j,3}} = \frac{\sigma_j}{\eta_{j,1}}, \quad \text{for all } j = 1, 2, \dots, N.$$

Then the stationary distribution, obtained by solving (65), is given by

$$p(v, \mathbf{u}, \mathbf{z}) = C \left(\prod_{j=1}^N \frac{1}{g_j'(g_j^{-1}(u_j))} \right) \exp \left[-\frac{v^2}{2\langle V^2 \rangle} - \sum_{j=1}^N \frac{1}{\sigma_j} G_j(g_j^{-1}(u_j)) - \sum_{j=1}^N \frac{2\eta_{j,2}}{\eta_{j,4}^2} H_j(z_j) \right], \quad (66)$$

where C is the normalization constant and functions G_j and H_j are integrals of functions g_j and h_j , respectively, which are given by

$$G_j(y) = \int_0^y g_j(\xi) d\xi, \quad H_j(y) = \int_0^y h_j(\xi) d\xi, \quad \text{for } j = 1, 2, \dots, N.$$

Following (37), we assume that $h_j(z_j) = z_j$ and each g_j is a function of one additional positive parameter $\eta_{j,5}$, $j = 1, 2, \dots, N$, given as

$$g_j(y) = |y|^{1/\eta_{j,5}} \text{sign } y. \quad (67)$$

Then we have,

$$g_j'(g_j^{-1}(u_j)) = \frac{|u_j|^{1-\eta_{j,5}}}{\eta_{j,5}} \quad \text{and} \quad G_j(g_j^{-1}(u_j)) = \frac{\eta_{j,5}}{1+\eta_{j,5}} |u_j|^{1+\eta_{j,5}}.$$

Then the stationary distribution (66) is Gaussian in V_i and $Z_{j,i}$ variables and we can integrate (66) to calculate the marginal distribution of $U_{j,i}$ by

$$p_j(u_j) = \int_{-\infty}^{\infty} \dots \int_{-\infty}^{\infty} p(v, \mathbf{u}, \mathbf{z}) dv du_1 du_2 \dots du_{j-1} du_{j+1} \dots du_N dz.$$

Consequently,

$$p_j(u_j) = C_j |u_j|^{\eta_{j,5}-1} \exp \left[-\frac{\eta_{j,5}}{\sigma_j(1+\eta_{j,5})} |u_j|^{1+\eta_{j,5}} \right], \quad (68)$$

where the normalization constant C_j is given

$$\int_{-\infty}^{\infty} p_j(u_j) du_j = 1.$$

Integrating (68), we can calculate

$$\langle |U_{j,i}|^\alpha \rangle = \int_{-\infty}^{\infty} |u_j|^\alpha p_j(u_j) du_j, \quad \text{for any } \alpha \geq 0,$$

As

$$\langle |U_{j,i}|^\alpha \rangle = \left(\frac{\sigma_j(1+\eta_{j,5})}{\eta_{j,5}} \right)^{\alpha/(1+\eta_{j,5})} \frac{\Gamma\left(\frac{\alpha+\eta_{j,5}}{1+\eta_{j,5}}\right)}{\Gamma\left(\frac{\eta_{j,5}}{1+\eta_{j,5}}\right)}. \quad (69)$$

The acceleration of the coarse-grained particle is given by

$$U_i = \sum_{j=1}^N U_{j,i}.$$

Using the symmetry of (68), odd moments of $U_{j,i}$ are equal to zero. In particular, $\langle U_{j,i} \rangle = 0$ and $\langle U_{3j,i} \rangle = 0$ for $j = 1, 2, \dots, N$. Consequently,

$$\langle U_i^2 \rangle = \sum_{j=1}^N \langle U_{j,i}^2 \rangle, \quad (70)$$

$$\langle U_i^4 \rangle = 3\langle U_i^2 \rangle^2 + \sum_{j=1}^N \langle U_{j,i}^4 \rangle - 3\langle U_{j,i}^2 \rangle^2, \quad (71)$$

which gives

$$\text{Kurt}[U_i] = \frac{\langle U_i^4 \rangle}{\langle U_i^2 \rangle^2} = 3 + \frac{\sum_{j=1}^N \langle U_{j,i}^4 \rangle - 3\langle U_{j,i}^2 \rangle^2}{\sum_{j=1}^N \langle U_{j,i}^2 \rangle^2}. \quad (72)$$

Substituting equation (69) for moments on the right hand side of equation (72), we can express the kurtosis of U_i in terms of $2N$ parameters σ_j and $\eta_{j,5}$, where $j = 1, 2, \dots, N$. For example, if we choose the values of dimensionless parameters $\eta_{j,5}$ equal to given numbers and define new parameters

$$\kappa_j = (\sigma_j)^{2/(1+\eta_{j,5})},$$

then equation (69) implies that $\langle U_{2j,i} \rangle$ is a linear function of κ_j and $\langle U_{4j,i} \rangle$ is a quadratic function of κ_j . Equations (70) and (71) can then be rewritten as the following system of two equations for $\kappa_1, \kappa_2, \dots, \kappa_N$

$$\sum_{i=1}^N c_{1,j} \kappa_j = \langle U_i^2 \rangle, \quad \sum_{i=1}^N c_{2,j} \kappa_j^2 = \langle U_i^4 \rangle - 3\langle U_i^2 \rangle^2,$$

where $c_{1,j}$ and $c_{2,j}$ are known constants, which will depend on our initial choice of values of $\eta_{j,5}$. Thus, using $N > 2$, we still have an opportunity to not only fit the second and fourth moments of the force distribution, but other moments as well. For example, the 6-th moment, $\langle U_i^6 \rangle$,

would include the linear combination of the third powers of k_j . We could also fit other properties of the force distribution estimated from MD simulations. For example, we could generalize one-parameter nonlinearities (67) to two-parameter nonlinear functions, as we did in equation (52). Then we could match the value of the distribution at $u = 0$, if our aim was to get a better fit of the MD acceleration distribution obtained in the illustrative example in Figure 2(b). Another possible generalization is to consider nonlinear functions h_j , provided that we estimate more statistics on the auxiliary variable Z from MD simulations.

conclusions

Equations (2)–(5) provide a family of SCG models that we have presented and examined. These models can be parametrized to fit the properties of detailed all-atom MD models. Erban (2016) created a multiscale (multi-resolution) technique that uses the linear SCG model (6)–(9), which is a specific choice of functions g_j and h_j in equations (2)–(5), as a transitional description between all-atom MD simulations and BD models. In Sections 2 and 3, the linear SCG model is examined in further detail. We point out that, as N increases, the $4N$ parameters of this model can more accurately match some statistics determined from all-atom MD simulations, but that, for all values of N , there are still statistics that cannot be matched. Non-Gaussian force distributions are among them.

References

Carof A, Vuilleumier R, Rotenberg B (2014) Two algorithms to compute projected correlation functions in molecular dynamics simulations. *Journal of Chemical Physics* 140(12):124103

Davtyan A, Dama J, Voth G, Andersen H (2015) Dynamic force matching: A method for constructing dynamical coarse-grained models with realistic time dependence. *Journal of Chemical Physics* 142:154104

Davtyan A, Voth G, Andersen H (2016) Dynamic force matching: Construction of dynamic coarse-grained models with realistic short time dynamics and accurate long time dynamics. *Journal of Chemical Physics* 145:224107

Dobramysl U, Rüdiger S, Erban R (2016) Particle-based multiscale modeling of calcium puff dynamics. *Multiscale Modelling and Simulation* 14(3):997–1016

Erban R (2014) From molecular dynamics to Brownian dynamics. *Proceedings of the Royal Society A* 470:20140036

Erban R (2016) Coupling all-atom molecular dynamics simulations of ions in water with Brownian dynamics. *Proceedings of the Royal Society A* 472:20150556

Erban R, Chapman SJ (2009) Stochastic modelling of reaction-diffusion processes: algorithms for bimolecular reactions. *Physical Biology* 6(4):046001

Erban R, Chapman SJ (2019) Stochastic Modelling of Reaction-Diffusion Processes. *Cambridge Texts in Applied Mathematics*. ISBN 9781108498128. Cambridge University Press

Farafonov V, Nerukh D (2019) MS2 bacteriophage capsid studied using all-atom molecular dynamics. *Interface Focus* 9:20180081

Flegg M, Chapman SJ, Erban R (2012) The two-regime method for optimizing stochastic reaction-diffusion simulations. *Journal of the Royal Society Interface* 9(70):859–868
Flegg M, Chapman SJ, Zheng L, Erban R (2014) Analysis of the

two-regime method on square meshes.
SIAM Journal on Scientific Computing
36(3):B561–B588

Kang M, Othmer H (2007) The variety of
cytosolic calcium responses and possible
roles of PLC and PKC. *Physical Biology*
4:325–343

Kang M, Othmer H (2009) Spatiotemporal
characteristics of calcium dynamics in
astrocytes. *Chaos* 19:037116

Kubo R (1966) The fluctuation-dissipation
theorem. *Reports on Progress in Physics*
29:255–284

Leimkuhler B, Matthews C (2015)
*Molecular Dynamics, Interdisciplinary
Applied Mathematics*, vol 39. Springer